Journal of Materials Science & Technology 32 (2016) 721–728

Contents lists available at ScienceDirect

Journal of Materials Science & Technology

journal homepage: www.jmst.org

Antibacterial Action of Chemically Synthesized and Laser Generated Silver Nanoparticles against Human Pathogenic Bacteria

Nosheen Zafar [1], Shahzadi Shamaila [1,*], Jawad Nazir [2], Rehana Sharif [1], Muhammad Shahid Rafique [1], Jalees Ul-Hasan [1], Syeda Ammara [1,3], Hina Khalid [1]

[1] Department of Physics, University of Engineering and Technology, Lahore 54890, Pakistan
[2] Department of Microbiology, University of Veterinary and Animal Sciences, Lahore, Pakistan
[3] Department of Physics, Forman Christian College, A Charted University, Lahore, Pakistan

ARTICLE INFO

Article history:
Received 5 June 2015
Received in revised form
23 November 2015
Accepted 27 November 2015
Available online 1 June 2016

Key words:
Chemically synthesized and laser ablated nanoparticles
UV-visible spectrophotometer
Gram negative and gram positive bacteria

Silver nanoparticles in the range of 10–40 nm were synthesized chemically and by laser ablation, employed for in vitro antibacterial action against human pathogenic bacterium. Their formation was evidenced by UV-visible spectrophotometer; particle size confirmed by atomic force microscopy, crystal structure determined by X-ray diffraction and chemical composition investigated by Fourier transform infrared spectroscopy. The calculated MIC (minimum inhibitory concentration) of chemically synthesized nanoparticles with 30–40 nm in size are 2.8 μg/mL, 4.37 μg/mL, 13.5 μg/mL and 2.81 μg/mL for *E. coli*, *S. aureus*, *B. subtillis* and *Salmonella*, respectively. Whereas laser ablated nanoparticles exhibit MIC of 2.10 μg/mL, 2.36 μg/mL and 2.68 μg/mL for *E. coli*, *S. aureus* and *Salmonella*, respectively.

1. Introduction

During the recent years, metallic nanoparticles have been widely used in the applications of biomedical field and in biotechnology[1]. Silver nanoparticles (Ag NPs) are proved to be a new engineering tool with remarkable unique characteristics and morphologies. Silver in the form of nanoparticles (especially in the range of 1–100 nm) exhibits ultra large surface area to volume ratio, so its synthesis and utilization is a competent area of scientific research. Unique interactions with virus and bacteria depend on different size ranges and shapes of Ag NPs[2]. During the past decades, Ag NPs have been famous for its bactericidal and inhibitory effects against various pathogens[3]. Due to their antibacterial activity, they can be applied in medical field for burn treatment[4,5], for catheters, protection of bacteria colonization[6,7], in textile fabrics[8,9] for water disinfection[10]. Besides that, AgNPs also exhibit a strong cyto-protective activity for infections of human immunodeficiency virus (HIV)[11]. Other applications are their unique optical and electronic properties with good chemical stability as a catalyst, in surface-enhanced Raman spectroscopy and electro analysis[12].

Numerous physical and chemical techniques have been used to synthesize AgNPs, such as photochemical method[13,14], laser ablated technique[15], micro emulsion[16], microwave treatment[17] and γ-irradiation method[18]. Parallel to these biosynthetic methods[19–21], physicochemical synthesis techniques[22] have also been widely used with the aim of improving the shape and size of AgNPs. Among these, the most versatile technique is the chemical technique[23–26], which requires only metallic precursors, reductants and finally stabilizing agents to prevent these nanoparticles from agglomeration. The size of the nanoparticles can be easily controlled by adjusting the quantity of metallic precursor.

Laser ablation technique in liquid environment is also another promising technique, which is easy to handle. It is a fast and easy production method, which does not require any vacuum and high temperature as the need of other laser techniques. Furthermore, no harmful and pyrophoric precursors are required for the synthesis of nanoparticles. So these nanoparticles can be easily used in biochemical or biotechnology for in vivo and in vitro applications[15].

Silver as nanoparticles is more toxic for bacteria as compared to its bulk form and highly reactive with strong catalytic properties. Small size nanoparticles (e.g., 10 nm)[13] may easily pass through cell wall, and cell malfunction occurs by the addition of intracellular nanoparticles. For direct measurement of microbial growth, serial dilution and disk diffusion are most dominated, while for indirect method, turbidity technique is employed. Indirect methods

* Corresponding author. Ph.D.; Tel.: +92 42 99029204; Fax: +92 42 99029415.
E-mail address: drshamaila.uet@gmail.com (S. Shamaila).

http://dx.doi.org/10.1016/j.jmst.2016.05.009

are easy and yield short time to investigate microbial activity. A spectrophotometer is used to measure the turbidity. The effect of Ag NPs on bacterial growth was investigated at 600 nm[27].

In the current research, pure Ag NPs have been produced by chemical method and pulsed Nd:YAG laser ablation from silver target in deionized water. The synthesized nanoparticles were investigated by various techniques such as UV-visible spectrophotometer, X-ray diffraction (XRD), atomic force microscopy (AFM) and Fourier transform infrared spectra (FTIR). These synthesized Ag NPs were applied to well-known four human pathogenic bacteria like *Escherichia coli* (*E. coli*), *Staphylococcus aureus* (*S. aureus*), *Bacillus subtillis* (*B. subtillis*) and *Salmonella*.

2. Experimental

2.1. Synthesis of chemically generated Ag NPs

Silver nitrate ($AgNO_3$), sodium borohydrate ($NaBH_4$) and deionized water were utilized in this experiment as received. Fabrication of Ag nanoparticles was done according to literature[28] by adding 0.001 mol/L silver nitrate solution (2 mL) drop wise (about 1 drop in 1 second) to 0.002 mol/L sodium borohydrate chilled solution (20 mL). Shake the solution in Erlenmeyer flask with a magnetic stirrer. As silver nitrate solution added, the solution immediately changed to light yellow color. The chemical reaction is:

$$2AgNO_3 + 2NaBH_4 + 6H_2O \rightarrow 2Ag^+ + 7H_2 + 2H_3BO_3 + 2NaNO_3 \quad (1)$$

The stirring process was continued for 1 min. If stirring sustained for long time after the addition of silver nitrate, aggregation started as the yellow solution first became darker yellow and then violet, and finally grayish resulting to precipitate formation of particles in the solution. After the completion of reaction, it was cooled at room temperature. Nanoparticles were separated by centrifugation, washed three times with deionized water and desiccated at room temperature.

2.2. Synthesis of laser ablated Ag NPs

Silver NPs were fabricated by laser ablation of the silver target immersed in the deionized water. The thickness of the target was 15 mm with 99.9% purity. Before starting the experiment, surface contaminations were removed with ethanol and water. A pulsed Nd:YAG laser (wavelength: 1064 nm), having energy 10 mJ/pulse and pulse length of 10 ns was subjected for the ablation. The target was dipped in deionized water. The laser operated at 10 Hz repetition rate with 1000 shots on first sample and 2000 shots on second sample. Laser irradiation on surface of target gives fast removal of the material from the confined laser spot. The synthesized nanoparticles changed the color of liquid demonstrating the formation of Ag NPs.

2.3. Antibacterial activity

A variety of techniques such as micro-dilution method[29], well diffusion method[30], serial dilutions method[15] and turbidity method[31] exist to provide a reliable prediction about a microorganism responding to antibiotics. In the current research, turbidity technique was utilized to ensure the antimicrobial action of Ag NPs against four human pathogenic bacteria containing two gram negative bacteria (*E. coli* and *Salmonella*) and two gram positive bacteria (*S. aureus* and *B. subtillis*). Then these antibacterial results are further evaluated by well diffusion method. In the literature[31], turbidity method has been employed to compare the antimicrobial action of Ag NPs with antibiotics[31]. Nutrient broth (Oxoid Ltd., Basingstoke, Hampshire, England) as a dehydrated powder was used to prepare the medium. Sterility of the medium was tested by incubating at 37 °C for 24 h.

An amount of 5.00 mL of the medium (nutrient broth) was dispensed in the tubes and sterilized by autoclaving at 121 °C for 15 min, thus making transparent broth media. The culture was prepared by transferring a known culture of gram positive bacteria (*S. aureus* and *B. subtillis*) and gram negative (*E. coli* and *salmonella*) into four tubes of broth medium with the help of a platinum wire. After inoculation, the tubes were placed in an incubator at 37 °C for 24 h, showing a visible growth in the culture tube. Low, medium and high doses of sterilized silver nanoparticle on the growth of bacteria were tested. Each tube was contained 5 mL of the medium, 200 μL of the inoculums with the required dose of the stock solution of nanoparticles. Triplicate tubes were prepared for each dose of Ag NPs. Negative control (broth and nanoparticles) and positive control (broth and inoculums) tubes were prepared along with and incubated at 37 °C for 24 h.

Turbidity of the medium in the inoculated tubes was checked in an Elisa reader/spectrophotometer with a filter of wavelength 600 nm. An amount of 200 μL of the sample was dispensed to each micro well plate and reading was taken accordingly. The optical density (OD) values given by ELISA (enzyme-linked immunosorbent assay) reader in absorption mode conceal the growth of bacteria in the sample. Triplicate OD values and their mean were taken for same sample along with standard deviation.

For well diffusion method, the nutrient Agar plates were prepared with four wells. The bacterial suspension of *S. aureus* and *E. coli* of 100 mL was uniformly applied on the upper surface of these plates. Then three low, medium and high doses of Ag NPs solutions were injected in these wells along with control. After incubated at 37 °C for 24 h, average diameter of the inhibition zone around each well for each bacterial disk was calculated with great precision. The mean and standard deviation (SD) with three replicates were taken for each microbial strain.

The synthesized Ag NPs have been analyzed by using various techniques including AFM for particle dimension, UV-visible spectroscopy for confirmation of surface plasmon response (SPR), XRD for structural analysis. The diffractogram has been observed in the 2θ range from 10° to 80°. FTIR has investigated in the region of 4000–400 cm^{-1}. For FTIR analysis, NPs were placed on KBr pellets in the form of drops from the solution of Ag NPs. The reflectance spectrum of diffused nanoparticles pellet was observed.

3. Results and Discussion

3.1. UV-visible spectroscopy of Ag NPs

The formation of silver colloidal solution is investigated by analyzing the absorption of Ag NPs by UV-visible spectroscopy. The absorption band of Ag NPs was analyzed in the range of 380–450 nm[32]. UV-visible SPR peaks for chemically synthesized Ag NPs are shown in Fig. 1. Fig. 1(a) exhibits absorption peaks at $\lambda \sim 402$ nm after 4 h and $\lambda \sim 405$ nm after 24 h of chemical synthesis and Fig. 1(b) indicates $\lambda \sim 405$ nm for 1000 shots and 2000 shots for laser ablated Ag NPs. Here, absorbance increases with increasing number of shots, indicating the increase in the concentration of Ag NPs.

As time increases for chemically generated Ag NPs, absorbance increases in particle concentration with slow enhancement in particles size range, indicating a red shift in SPR spectra. While SPR spectra of laser ablated Ag NPs do not exhibit any shift with increasing number of shots, indicating the increase in particle concentration only.

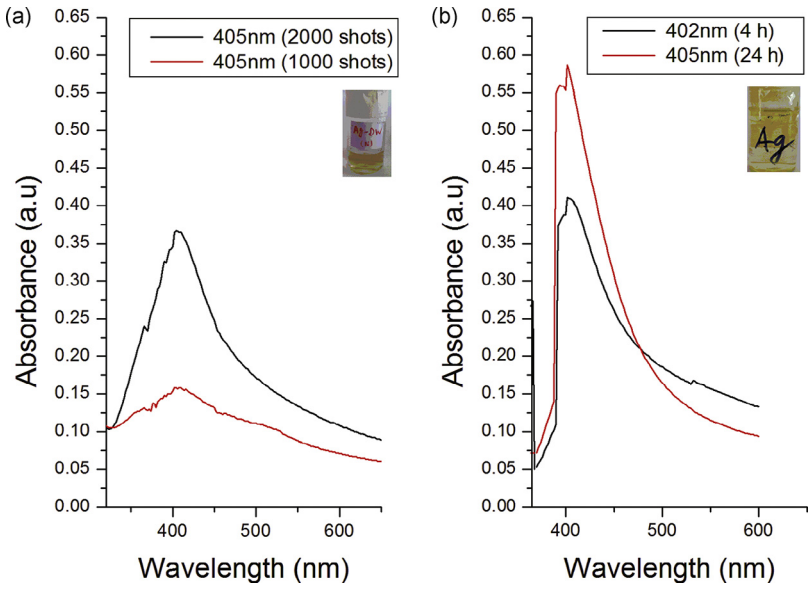

Fig. 1. (a) UV-visible spectroscopy of laser ablated Ag NPs (λ ~ 405 nm) for 1000 shots and (λ ~ 405 nm) for 2000 shots; (b) UV-visible spectroscopy of chemically synthesized Ag NPs for (λ ~ 402 nm) after 4 h and (405 nm) after 24 h.

3.2. AFM analysis of Ag NPs

The Ag NPs for AFM analysis were deposited on the silicon chips. The tapping mode was utilized to get AFM images of nanoparticles. The two dimensional (2D) images with scan area (1 μm × 1 μm) and histogram of chemically synthesized nanoparticles are shown in Fig. 2(a) and (b) while laser ablated Ag NPs are shown in Fig. 2(c–f). The size of chemically synthesized Ag NPs ranges from 20 nm to 40 nm as indicated by the histogram. The maximum particle size range is 25 to 35 nm.

The histogram of laser ablated Ag NPs with 1000 shots shown in Fig. 2(c) and (d) indicates particle size in the range of 20 to 35 nm. The maximum numbers of particles are found in the range of 25–30 nm. Here, particle concentration is very low as revealed by Fig. 2(c).

Fig. 2(e) and (f) reveals the 2D topographic images of laser ablated Ag NPs after 2000 shots and histogram curve, respectively. The size of Ag NPs is in the range of 10–35 nm as indicated by the histogram. The range of maximum number of particles is 20–30 nm.

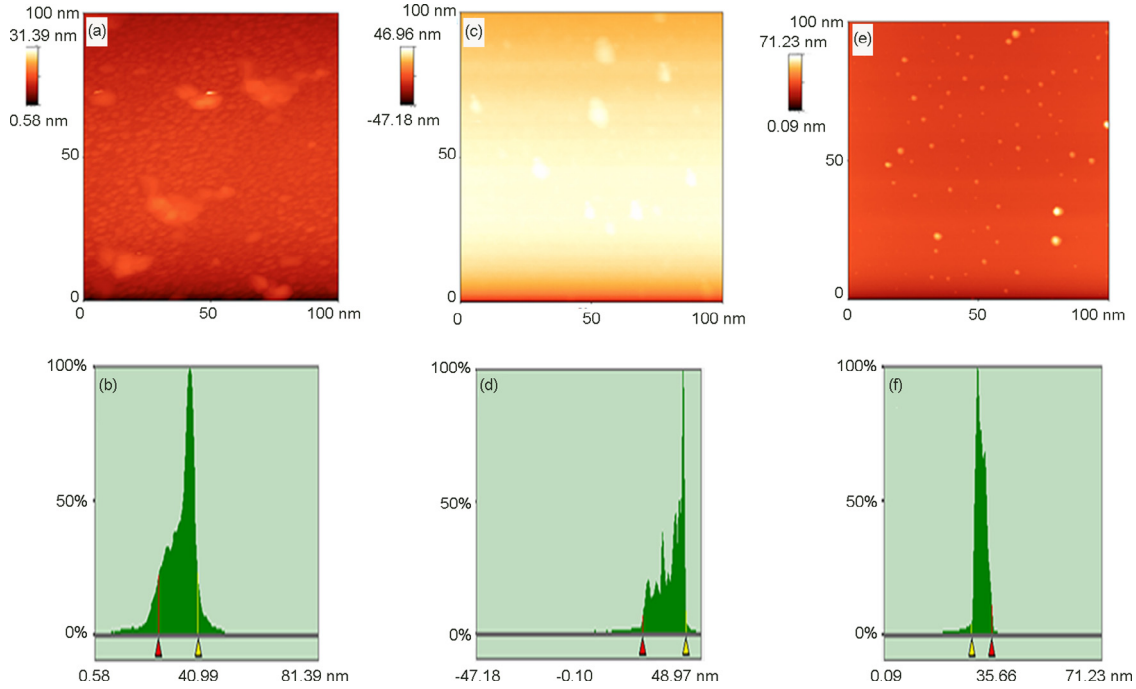

Fig. 2. AFM image: (a and b) of two dimensional (2D) image and histogram of chemically synthesized nanoparticles after 24 h; (c and d) 2D and histogram of laser ablated Ag NPs sample for 1000 shots; (e and f) 2D and histogram of laser ablated Ag NPs sample for 2000 shots.

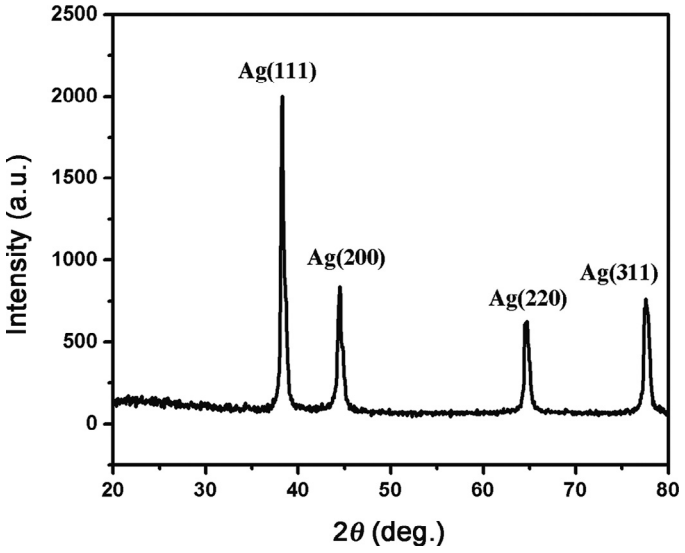

Fig. 3. XRD pattern of Ag NPs synthesized by chemical reduction method.

AFM analysis reveals the comparison in both techniques. Laser ablated nanoparticles are precise, well dispersed and spherical but in low concentration, while chemically generated nanoparticles are in abundance but exhibit slightly large size range.

3.3. XRD analysis of chemically synthesized Ag NPs

The crystal structure of Ag NPs has poly crystalline face centered cubic structure analyzed by XRD. Appearance of (111) peak in Fig. 3 reveals the antibacterial performance of Ag NPs[33].

3.4. XRD analysis of laser ablated Ag NPs

The XRD pattern of Ag NPs generated by laser ablation is shown in Fig. 4. Diffraction peaks are indexed identical to XRD pattern of chemically generated Ag NPs. Thus, these Ag NPs have polycrystalline structure with various preferred orientations and only difference is the peaks intensity. This evaluates the less particle concentration of laser ablated Ag NPs[34].

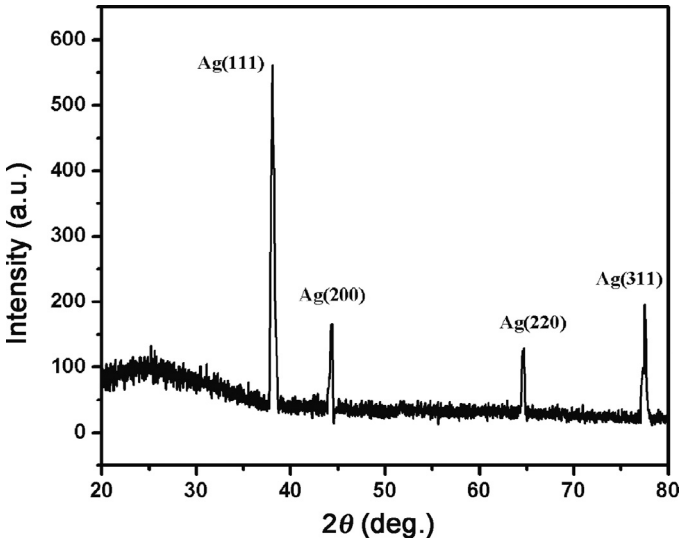

Fig. 4. XRD pattern of Ag NPs synthesized by laser ablation method.

3.5. FTIR analysis of Ag NPs

FTIR spectroscopy recognizes the chemical composition of the surface of Ag NPs. The FTIR spectra of deionized water and chemically synthesized Ag NPs are shown in Fig. 5. The water molecules, incorporated into the lattice structure of a crystalline compound gives sharp bands in the regions of 3800–3200 cm^{-1} and 1700–1600 cm^{-1}, due to O—H stretching and bending, respectively[35]. So in FTIR spectra of Ag NPs, three peaks appears at 3855 cm^{-1}, 3793 cm^{-1} and 3614 cm^{-1} due to O—H stretching. Peak at 2348 cm^{-1} represents B—H stretching. The broad absorption of hydroxyl group (O—H) of deionized water appears at 3266 cm^{-1} and 3219 cm^{-1} before and after formation of nanoparticles, respectively, indicating 47 units blue shift. Here, inter and intra-molecular bonds of hydrogen are responsible for this broadening of the O—H band. This enhancement in wave number may happen due to less interaction of Ag NPs with group of O—H band. The bond observed before formation of nanoparticles at 1639 cm^{-1} and shifting after formation of nanoparticles at 1638 cm^{-1} indicates C═C stretching having less co-ordination with Ag NPs[35].

A broad peak at 3426.89 cm^{-1} in FTIR analysis of Ag NPs indicate the OH stretching as shown in Fig. 6. The other peaks, observed at 1044, 1129, 1233 and 1464 cm^{-1}, are assigned to the stretching modes of (CO_3) called carbonato complexes synchronized to a metal surface. So indication of these groups on the Ag NPs surface revealed the presence of Ag—O compounds[36].

3.6. Antimicrobial activity of Ag NPs

The antibacterial activity (in vitro) of the samples was evaluated by using the turbidity method using nutrient broth with determination of inhibition zones by taking optical density (OD) values of spectrophotometer.

The three doses were designed, in which low, medium and high dose solutions contain 0.784 μg, 1.57 μg, 2.35 μg of Ag NPs, respectively.

The mean optical density (OD) values of all 24 test tubes were carefully observed. Antimicrobial activity of Ag NPs on *S. aureus*, *E. coli*, *B. subtillis* and *Salmonella* was demonstrated. Bacteria in nutrient broth (positive control) reveal the growth of bacteria. The percentage increase or decrease in bacterial growth was calculated against OD value of pure nutrient broth media (reference OD value).

The OD value of broth media and inoculums help us to calculate the percentage growth of *S. aureus* and *E. coli* after 24 h incubation time at 37 °C. The maximum growth of *S. aureus*, *E. coli*, *B. subtillis* and *Salmonella* was 75.19%, 74.3%, 68.5% and 71.9%, respectively. Growth by contaminant microorganisms was 1.5%, which is ignorable against 74.2% or 74.3% or 68.5% or 71.9% growth.

The difference of OD value of dose effected culture and pure nutrient broth give the OD value of culture growth inhibition. The growth of bacteria decreases with increasing dose of nanoparticles (Table 1).

Chemically synthesized Ag NPs inhibited *S. aureus* up to 67.02%, whereas *E. coli* inhibited up to 87.9%. It means that more doses are required for complete inhibition of *S. aureus*. Growth inhibition of *B. subtillis* was only 39.9% and *Salmonella* inhibited only 80.2%. While laser ablated Ag NPs inhibited these bacterium with greater efficiency and with low dose such as *S. aureus* inhibited up to 92.0%, whereas *E. coli* completely inhibited and growth inhibition of *Salmonella* is 82.0% (Fig. 7).

Two types of Ag NPs were synthesized. The size of chemically synthesized nanoparticles were in the range of 30–40 nm while the size range of laser ablated nanoparticles were 20–30 nm, slightly smaller than the former one. The same doses of laser ablated nanoparticles provide maximum inhibition against each pathogen.

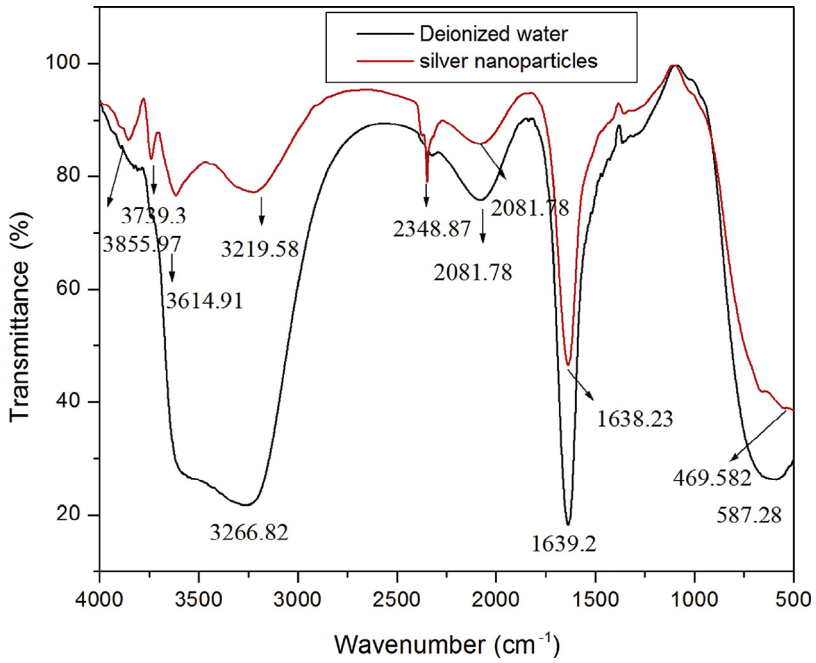

Fig. 5. FTIR spectra of deionized water and Ag NPs synthesized by chemical reduction method.

Chemically synthesized nanoparticles are proved to be less efficient as compared to laser ablated due to adsorption of some chemical species on its surface, which produced adverse effect in antibacterial action. This indicates that the chemical reduction technique is favorable for the preparation of the nanocolloids but the growth of nanocrystals depends on its ligands. Hence, for the purity of sample, chemical reduction has various restrictions to utilize these NPs for the catalytic, biological and sensing applications.

Laser ablation technique is a powerful technique to synthesize a variety of metallic nanoparticles[15,37]. This technique produces NPs in liquid in the form of stable colloidal solution, which can be easily collected. The high stability of the colloidal solutions is due to charging

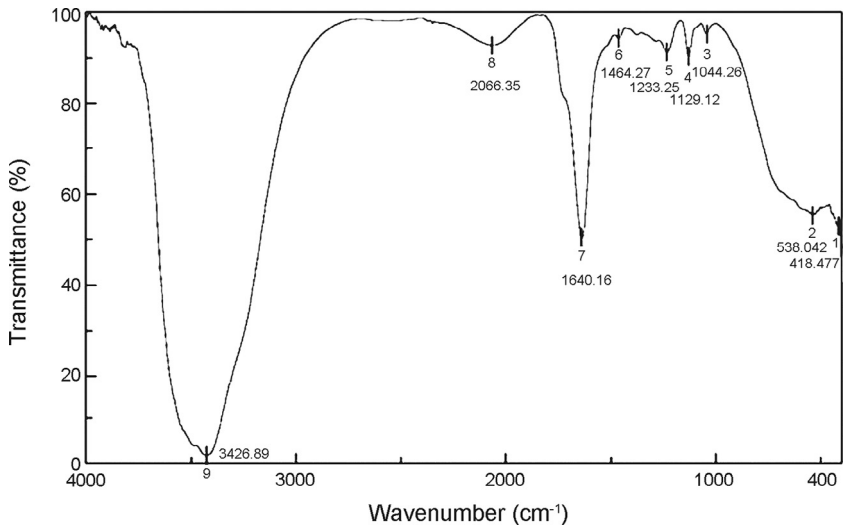

Fig. 6. FTIR spectrum of Ag NPs synthesized by laser ablated method.

Table 1
Effect of low (0.78 μg/mL), medium (1.57 μg/mL) and high (2.35 μg/mL) dose on growth inhibited (%) *S. aureus*, *E. coli*, *B. subtilis* and *Salmonella*

Strain	Chemically synthesized Ag nanoparticles			Laser ablated Ag nanoparticles		
	Low dose	Medium dose	High dose	Low dose	Medium dose	High dose
S. aureus	41.5 ± 0.5	53.8 ± 1.7	67.02 ± 0.9	52.3 ± 0.5	76.3 ± 1.7	92.0 ± 0.9
E. coli	46.81 ± 1.7	63.2 ± 0.9	87.9 ± 0.9	57.1 ± 1.7	84.5 ± 0.9	99.81 ± 0.9
Salmonella	38.1 ± 0.2	58.9 ± 0.2	80.2 ± 0.2	40.5 ± 0.2	68 ± 0.2	82 ± 0.2
B. subtillis	31.5 ± 0.3	33.7 ± 0.3	39.9 ± 0.3	–	–	–

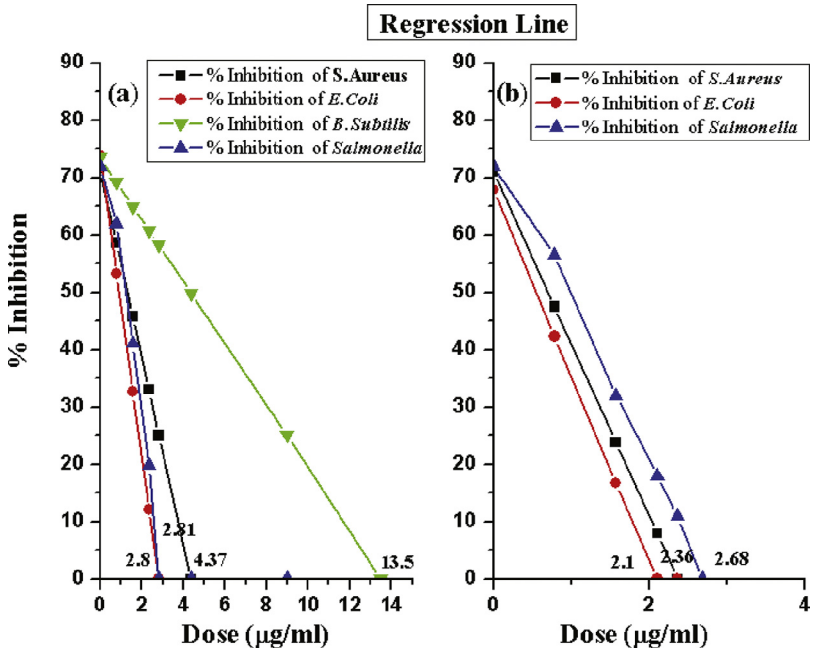

Fig. 7. (a) Growth inhibition of *S. aureus*, *E. coli*, *B. subtilis* and *Salmonella* by chemically synthesized Ag NPs; (b) growth inhibition of *S. aureus*, *E. coli* and *Salmonella* by laser ablated Ag NPs according to regression line.

of nanoparticles as the atoms of the surface are oxidized. These nanoparticles are produced by the interaction of the vapor of liquid with the metallic surface of target; hence, the resultant colloids are extremely pure. Main advantage of this method is the colloid stability and size of nanoparticle, which can be easily controlled by choosing the suitable conditions, i.e., laser wavelength, its frequency, fluence, time for pulse duration and ablation, light focusing techniques and surface of target. The only disadvantage of this technique is the low concentration of nanoparticles in the colloid due to laser irradiation's absorption and scattering by suspension[37].

Antimicrobial action of Ag NPs depends on the properties of bacterial species. The main difference between gram positive and gram negative bacterium is the membrane structure, i.e., the thickness of the peptidoglycan layer, which is only present in pathogenic bacteria. It contains polymer with sugar and amino acid, making an outside of plasma membrane, i.e., cell wall, and provides structural strength counteracting the cytoplasm osmotic pressure. Its thickness is 50% in Gram positive bacteria and 8% in Gram negative bacteria. Thus, Gram positive bacteria has multiple peptidoglycan layer with no outer membrane and lipo-polysacchraride but a long chain of teichoic acids. On the other hand, Gram negative bacteria have a thin and single layer of peptidoglycan with no teichoic acid. Outer membrane has lipo-polysacchraride and periplasmic space along with outer membrane. However, its outer membrane is made of tightly packed molecules of lipo-polysacchraride, which affect as efficient resistive barrier[38].

The colloidal fluid of nanoparticles having Ag^+ in the nutrient broth media may join itself to the cell wall of negatively charged bacterium and penetrate, leading to denaturation of protein and causes cell death. The attachment of silver ions and nanoparticles to the bacterium cell wall exhibits accumulation of protein precursor's layer, which finally deactivate the proton motive force. Ag NPs cause outer membrane destabilization and crack the plasma membrane, thus damaging the depletion of intracellular ATP (adenosine triphosphate)[39].

Concentration and size of nanoparticles play an important role in the antibacterial action. The results in the literature[40] revealed that antibacterial action of Ag NPs upon gram-negative bacteria is dependent on the particles' concentration and strongly linked with the progress of holes produced in the bacteria's cell wall. Shrivastava et al.[41] reported that the effect of Ag NPs on *S. aureus* is much less. *B. subtillis* has been proved to be the most powerful gram positive bacteria because it has its own strategy for its survival in any harsh conditions. Its survival is the production of endospores (stress-resistant), and its external DNA uptake process which can be occurred by the recombination with original DNA (called DNA duplex). At the same time, it can be more protective under harsh situations, i.e., alkaline, acidic, oxidative or osmotic conditions, and in high heat. *Salmonella* is also more resistive gram negative bacteria as compared to *E. coli*.

In recent research, Ag NPs showed higher antibacterial effect against *E. coli* with respect to other observed bacteria. *S. aureus* is more resistive than *E. coli*; therefore a high dose of 2.10 µg/mL is enough for maximum inhibition of *E. coli*. Due to thicker peptidoglycan layer of gram positive bacteria, more doses of Ag nanoparticles are required for complete inhibition of *S. aureus* and *Salmonella*.

The laser ablated Ag NPs have showed high antibacterial activity, which may be utilized in coatings, wood flooring and cotton textiles.

3.7. Statistical analysis

Dose value of Ag NPs for maximum growth inhibition of bacteria was estimated by statistical analysis (regression line), and the standard error for estimated value has also been calculated. All the tests were done in triplicate, independently. However, all experimental data were analyzed by using Student's *t*-test with $p < 0.05$.

3.8. Regression line

For regression line, dose of Ag NPs has independent variable *X*, whereas percentage growth has dependent variable *Y*. Regression line has been calculated by substituting the variables' value from Table 1 in the equations below:

Table 2
Zone of inhibition (mm) for low (0.78 μg/mL), medium (1.57 μg/mL) and high (2.35 μg/mL) dose of chemically synthesized and laser ablated Ag NPs on *S. aureus* and *E. coli*

Strain	Chemically synthesized Ag nanoparticles			Laser ablated Ag nanoparticles		
	Low dose	Medium dose	High dose	Low dose	Medium dose	High dose
S. aureus	11 ± 0.2	12 ± 0.3	13 ± 0.2	11 ± 0.5	13 ± 0.2	15 ± 0.3
E. coli	16 ± 1.7	19 ± 0.9	21 ± 0.9	18 ± 1.7	21 ± 0.3	23 ± 0.2

$$b = \frac{\sum XY - \frac{\sum X \sum Y}{N}}{\sum X^2 - \frac{(\sum X)^2}{N}} \quad (2)$$

$$a = \frac{\sum Y}{N} - b\frac{\sum X}{N} \quad (3)$$

$$Y = a + bX \quad (4)$$

From the above calculation, growth inhibition curves were obtained for both types of nanoparticles.

From the regression line in Fig. 7, the calculated MIC of chemically synthesized nanoparticles with 30–40 nm in size are 2.8 μg/mL, 4.37 μg/mL, 13.5 μg/mL and 2.81 μg/mL for *E. coli*, *S. aureus*, *B. subtillis* and *Salmonella*, respectively. Whereas laser ablated nanoparticles with 20–30 nm exhibit MIC of 2.10 μg/mL, 2.36 μg/mL and 2.68 μg/mL for *E. coli*, *S. aureus* and *Salmonella*, respectively.

The results of well diffusion method are represented in Fig. 8 and Table 2, which clearly demonstrate the zone of inhibition for chemically synthesized and laser ablated Ag NPs, which is absent in the control. Furthermore, the zone of inhibition of laser ablated NPs are slightly larger than that of chemically synthesized Ag NPs as listed in Table 2.

Kelmani et al.[42] reported the MIC of 3 μg/mL, 12 μg/mL and 11 μg/mL of Ag NPs (51 nm in size) for *E. coli*, *S. aureus* and *Salmonella*, respectively, through serial dilution method. Raffin et al.[43] observed that Ag NPs with mean sizes of 16 nm were completely cytotoxic for *E. coli* at a low concentration. Jozani et al.[44] fabricated Ag NPs by green synthesis in the size range of 10–20 nm, for which MIC was 3.1 μg/mL, 12.5 μg/mL and 12.5 μg/mL for *E. coli*, *S. aureus* and *Salmonella*, respectively, obtained by serial dilution method. Vanaja et al.[45] fabricated Ag NPs by biosynthesis method in 2–10 nm range of nanoparticles and maximum zone of inhibition was obtained for *E. coli* as compared to *Salmonella* and minimum for *B. subtillis*. Ag NPs size plays a vital role in antimicrobial performance[13,46]. Ag NPs of 29 nm size observed MIC's 13 and 17 μg/mL against *E. coli* and *S. aureus*, respectively[47].

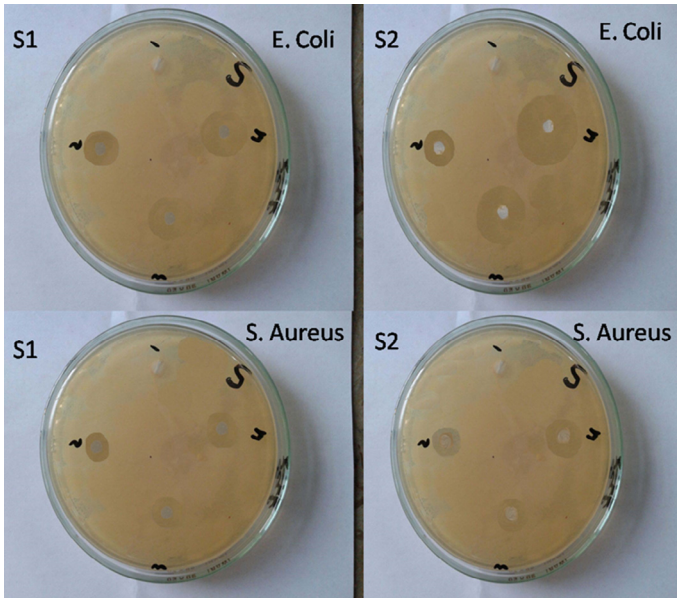

Fig. 8. Well diffusion method of two sized Ag NPs against *E. coli* and *S. aureus*.

4. Conclusion

The chemically synthesized and laser ablated Ag NPs in this research project exhibited stronger antibacterial activity than those reported earlier[13,46,47]. The activity was size and dose dependent and was more explicit against gram negative bacterium than gram positive ones. The fabricated nanoparticles are spherical in shape with polycrystalline nature having 10–40 nm in size, and exhibit absorption spectrum at 405 nm. Antibacterial effect of Ag NPs against four pathogenic bacteria reveals that Ag NPs are powerful antibacterial tool. The calculated MIC (minimum inhibitory concentration) of chemically synthesized nanoparticles with 30–40 nm in size are 2.8 μg/mL, 4.37 μg/mL, 13.5 μg/mL and 2.81 μg/mL for *E. coli*, *S. aureus*, *B. subtillis* and *Salmonella*, respectively. Whereas laser ablated nanoparticles with 20–30 nm exhibit MIC of 2.10 μg/mL, 2.36 μg/mL and 2.68 μg/mL for *E. coli*, *S. aureus* and *Salmonella*, respectively. These nanoparticles provide more physical, catalytic and chemical performance due to its larger surface area to volume ratio. Turbidity is proved to be a fast and efficient technique of estimating the presence of bacteria in a liquid. These MIC calculations are further helpful in calculating zone of inhibition by Agar diffusion method. The current research could be ready to lend a hand to the fields of environment, health, information technology, food department and cosmetics. Furthermore, Ag NPs have demonstrated safer life due to their flexible nature as compared to conventional antibiotics.

Acknowledgments

The authors highly obliged the Physics and Polymer Department (University of Engineering and Technology, Lahore), Physics Department (COMSATS institute, Lahore) and Chemistry Department (Forman Christian College, A Charted University, Lahore) for facilitating the service of AFM, FTIR, XRD and UV-visible spectrophotometer analysis, respectively. Furthermore, appreciation is given to the assistance of the Department of Microbiology, University of Veterinary and Animal Sciences, Lahore, Pakistan for antibacterial analysis.

References

[1] A.K. Bhunia, P.K. Samanta, D. Aich, S. Saha, T. Kamilya, J. Phys. D Appl. Phys. 48 (2015) 235305.
[2] P.V. Dong, C.H. Ha, L.T. Binh, J. Kasbohm, Int. Nano Lett. 2 (2012) 1–9.
[3] K. Shameli, M.B. Ahmad, S.D. Jazayeri, P. Shabanzadeh, P. Sangpour, H. Jahangirian, Y. Gharayebi, Chem. Cent. J. 6 (2012) 73.
[4] K. Singh, M. Panghal, S. Kadyan, U. Chaudhary, J.P. Yadav, J. Nanomed. Nanotechnol. 5 (192) (2014) 1–6.
[5] C. Rig, L. Ferroni, I. Tocco, M. Roman, I. Munivrana, C. Gardin, W.R.L. Cairns, V. Vindigni, B. Azzena, C. Barbante, B. Zavan, Int. J. Mol. Sci. 14 (2013) 4817–4840.
[6] M.E. Rupp, T. Fitzgerald, N. Marion, V. Helget, S. Puumala, J.R. Anderson, P.D. Fey, Am. J. Infect. Control 32 (8) (2004) 445–450.

[7] U. Samuel, J.P. Guggenbichler, Int. J. Antimicrob. Agents 23 (2004) S75–S78.
[8] T. Yuranova, A.G. Rincon, A. Bozzi, S. Parra, C. Pulgarin, P. Albers, J. Kiwi, J. Photochem. Photobiol. A Chem. 161 (2003) 27–34.
[9] H.Y. Lee, H.K. Park, Y.M. Lee, K. Kim, S.B. Park, Chem. Commun. (2007) 2959–2961.
[10] Q. Li, S. Mahendra, D.Y. Lyon, L. Brunet, M.V. Liga, D. Li, P.J.J. Alvarez, Water Res. 42 (2008) 4591–4602.
[11] J. Wu, Y. Zheng, X. Wen, Q. Lin, X. Chen, Z. Wu, Biomed. Mater. 9 (2014) 035005.
[12] A. Lopez-Miranda, A. Lopez-Valdivieso, G. Viramontes-Gamboa, J. Nanopart. Res. 14 (2012) 1101.
[13] J.R. Morones, J.L. Elechiguerra, A. Camacho, K. Holt, J.B. Kouri, J.T. Ramirez, M.J. Yacaman, Nanotechnology 16 (2005) 2346–2353.
[14] K. Mallick, M.J. Witcomb, M.S. Scurrell, J. Mater. Sci. 39 (2004) 4459–4463.
[15] S. Shamaila, H. Wali, R. Sharif, J. Nazir, N. Zafar, M.S. Rafique, Appl. Phys. Lett. 103 (2013) 153701.
[16] J.N. Solanki, Z.V.P. Murthy, Colloids Surf. A Physicochem. Eng. Asp. 359 (2010) 31–38.
[17] B. Kumar, K. Smita, L. Cumbal, A. Debut, R.N. Pathak, Bioinorg. Chem. Appl. (2014) 784268.
[18] H.S. Shin, H.J. Yang, S.B. Kim, M.S. Lee, J. Colloid Interface Sci. 274 (2004) 89–94.
[19] A.J. Kora, S.R. Beedu, A. Jayaraman, Org. Med. Chem. Lett. 2 (2012) 17.
[20] I.K. Sen, A.K. Mandal, S. Chakraborti, B. Dey, R. Chakraborty, S.S. Islam, Int. J. Biol. Macromol. 62 (2013) 439–449.
[21] A.M. Awwad, N.M. Salem, A.O. Abdeen, Int. J. Ind. Chem. 4 (2013) doi:10.1186/2228-5547-4-2.
[22] M. Dawy, H.M. Rifaat, S.A. Moustafa, H.A. Mousa, Aust. J. Basic Appl. Sci. 6 (3) (2012) 257–262.
[23] J. Liu, X. Li, X. Zeng, J. Alloys Compd. 494 (2010) 84–87.
[24] Z. Khan, S.A. Al Thabaiti, A.Y. Obaid, A.O. Al Youbi, Colloids Surf. B Biointerfaces 82 (2011) 513–517.
[25] M. Guzman, J. Dille, S. Godet, Nanomedicine 8 (2012) 37–45.
[26] J.I. Hussain, S. Kumar, A.A. Hashmi, Z. Khan, Adv. Mater. Lett. 2 (2011) 188–194.
[27] W.R. Li, X.B. Xie, Q.S. Shi, H.Y. Zeng, Y.S.O. Yang, Y.B. Chen, Appl. Microbiol. Biotechnol. 85 (2010) 1115–1122.
[28] J.S. Kim, E. Kuk, K.N. Yu, J.H. Kim, S.J. Park, H.J. Lee, S.H. Kim, Y.K. Park, Y.H. Park, C.Y. Hwang, Nanomedicine (2007) 95–101.
[29] L. Scorzoni, T. Benaducci, A.M.F. Almeida, D.H.S. Silva, V.S. Bolzani, M.J.S.M. Giannini, J. Basic Appl. Pharm. Sci. 28 (1) (2007) 25–34.
[30] R. Mie, M.W. Samsudin, L.B. Din, A. Ahmad, N. Ibrahim, S.N.A. Adnan, Int. J. Nanomed. 9 (2014) 121–127.
[31] F.R. Lourenço, T.D.J.A. Pinto, Braz. J. Pharm. Sci. 47 (2011) 573–584.
[32] D.K. Bhui, H. Bar, P. Sarkar, G.P. Sahoo, S.P. De, A. Misra, J. Mol. Liq. 145 (2009) 33–37.
[33] V.V. Shinde, P.R. Jadhav, J.H. Kim, P.S. Patil, J. Mater. Sci. 48 (24) (2013) 8393–8401.
[34] D. Dorranian, S. Tajmir, F. Khazanehfar, Soft Nanosci. Lett. 3 (2013) 93–100.
[35] B.H. Stuart, Infrared Spectroscopy: Fundamentals and Applications, John Wiley & Sons, 2004, pp. 46–50.
[36] J.P. Sylvestre, S. Poulin, A.V. Kabashin, E. Sacher, M. Meunier, J.H.T. Luong, J. Phys. Chem. B 108 (2004) 16864–16869.
[37] A.M. Brito-Silva, L.A. Gómez, C.B. de Araújo, A. Galembeck, J. Nanomater. (2010) 1–7.
[38] M. Umadevi, T. Rani, T. Balkrishnan, R. Ramanibai, Int. J. Pharm. Sci. Nanotechnol. 4 (2011) 1491–1496.
[39] M. Valodkar, S. Modi, A. Pal, S. Thakore, Mater. Res. Bull. 46 (2011) 384–389.
[40] I. Sondi, S. Sondi, J. Colloid Interface Sci. 275 (2004) 177–182.
[41] S. Shrivastava, T. Bera, A. Roy, G. Singh, P. Ramachandrarao, D. Dash, Nanotechnology 18 (2007) 225103.
[42] R.K. Chandrakanth, C. Ashajyothi, A.K. Oli, C. Prabhurajeshwar, Orient. J. Chem. 30 (2014) 1253–1262.
[43] M. Raffin, F. Hussain, T.M. Bhatti, J.I. Akhter, A. Hameed, M.M. Hasan, J. Mater. Sci. Technol. 24 (2008) 192–196.
[44] M.B. Jozani, M. Khatibzadeh, A. Hashemi, Proceedings of the International Conference Nanomaterials: Applications and Properties, vol. 3, 2014, pp. 1–5.
[45] M. Vanaja, K. Paulkumar, G. Gnanajobitha, S. Rajeshkumar, C. Malarkodi, G. Annadurai, Int. J. Metals (2014) Article ID 692461.
[46] C.N. Lok, C.M. Ho, R. Chen, Q.Y. He, W.Y. Yu, H. Sun, P.K.H. Tam, J.F. Chiu, C.M. Che, J. Biol. Inorg. Chem. 12 (2007) 527–534.
[47] G.A.M. Castañón, N.N. Martínez, F.M. Gutierrez, J.R.M. Mendoza, F. Ruiz, J. Nanopart. Res. 10 (2008) 1343–1348.